Low Percolation Behaviour of Polystyrene Carbon Nanoparticles (PS/CNPs) Composite

S.S. Ibrahim [1,2]

[1] *Cairo University, Faculty of Science, Physics Dep. Giza, Egypt*
[2]*Current address: King Faisal University, College of Science, Physics Dep,. Hofof, KSA*

Abstract

Polystyrene-Carbon nanoparticles (PS/CNPs) nanocomposites were fabricated via simple cast technique. The nanocomposite characterization involved morphological, optical, electrical and thermal properties using electron microscopy, UV-vis spectroscopy, dielectric spectroscopy, electrical conductivity and DSC analysis. Interesting results were obtained, as conductivity at low loadings of CNP in polystyrene matrix (0.08 volume ratio), nonlinear IV characteristic curves below and above percolation threshold, increase of dielectric permittivity with increasing CNPs loading near the percolation threshold, shift in T_g to higher temperature with loading CNP. SEM results were also discussed.

Key words: PS/CNPs, Nanocomposite, Dielectric Study, Percolation , UV-vis Analysis, DSC.

1. Introduction

Composites are a class of materials consisting of a mixture of two or more components to produce a multiphase system with different physical properties obtained from the constituents [1]. In carbon-nanocomposite, one of the phases is carbon, in some form, and it is generally introduced to impart certain functionality or to improve a certain behaviour of the composite. Carbon-nanocomposite or carbon filled polymeric composite generally have improved electrical and mechanical properties due to the incorporation of the carbon particles on the surface or into directly fiber. The carbon nanocomposite can be used in many applications such as static dissipation [2], electromagnetic shielding [3-6], and radio frequency interference [7], where low to moderate conductivity is acceptable. The enhanced mechanical properties can be useful in applications such as aerospace and defense where weight and mechanical properties are critical.

The interest in carbon filled polymeric materials have been renewed with the advent of nanostructure such as carbon nanotubes for use as multifunctional material due to its remarkable electrical, thermal and mechanical properties. Additionally, with these additives composite properties can be significantly enhanced at much lower loadings [8, 9]. Among the available fillers, carbon nanoparticle (CNP) and carbon nanotubes (CNT) have been used extensively due to their ability to impart high electrical conductivity to a polymer matrix at relatively low filler content [9-13]. CNP has been used widely in conventional polymer composites due to their relative advantages of low cost, small particle size (high surface area), and aggregation behaviour. CNP filled polymer composites in film form have been investigated for various applications including sensors [13], electrodes [14], and electromagnetic interference shielding [15].

Performance of composites depends on the characteristics of the filler, but also on its dispersion, filler-filler interaction and polymer-filler interactions, and more specifically on the properties and thickness of the polymer inter-phase between fillers [16]. In the case of conducting fillers, it is well known that the final electrical properties of the composites depend upon the capabilities of charge transmission from conducting filler to another.

Addition of CNP to PS increases the electrical conductivity due to the bridging of uninterrupted length of the conductive paths and the strength of the percolated filler network and, hence, the level of conductivity. This synergistic effect has been reported in many other studies [16-18].

2. Theoretical background

Percolation Model: The electrical conductivity of mixtures of conductive and insulating materials is generally dependent on the formation of the conductive network through the medium. To understand this network formation, many percolation models and equations have been proposed. Statistical percolation model basically deals with the probability of particle contacts within the medium. Two of early percolation models often referenced are the models proposed by Kirkpatrik [19] and Zallen [20]. The model followed a power law equation of the following form:

$$\sigma = \sigma_c (V - V_c)^t \quad for \ V > V_c \tag{1}$$

where σ_c is conductivity of the conducting component, υ is its volume fraction, t is a critical exponent, and υ_c is the critical volume fraction. The values of σ_c depend on the dimensions of the lattice.
The volume fraction for the composite sample will be calculated depending on the weight and densities of the constituents using the following equation:

$$\phi = \frac{\dfrac{W_{CB}}{\rho_{PS}}}{\dfrac{W_{CB}}{\rho_{PS}} + \dfrac{(1 - W_{CB})}{\rho_{CB}}} \tag{2}$$

ii-Dielectric Characterization:
Dielectric characterization is broadly based on the degree to which the electrical properties of a nanostructure of dielectric constant, ε_r, and thickness, d, depart from those of an ideal parallel plate capacitor, the capacitance (per area) of which is given by:

$$c = \frac{\varepsilon_r \varepsilon_o}{d} \tag{3}$$

where ε_o is the dielectric permittivity of free space (= 8.85 10^{-2} Fm^{-1}). Real capacitors leak electric charge with a characteristic time constant given by [34]:

$$\tau = \frac{c}{g} \tag{4}$$

Where g denotes the leak conductance, which is zero for an ideal capacitor. The reciprocal time constant yields a characteristic frequency given by:

$$\omega_{cons\tan t} = \frac{g}{c} \tag{5}$$

$$f_{cons\tan t} = \frac{\omega_{cons\tan t}}{2\pi} = \frac{g}{2\pi c} \tag{6}$$

below which the electrical properties are dominated by the leak conductance.

3. Experimental

3.1   DC conductivity and I-V Characterization
The electrical conductivity of the composite and pure film was measured at ambient temperature using the standard plate capacitor technique. The technique mentioned in previous work [21]. The conductivity σ was calculated from the following equation,

$$\sigma = \frac{Id}{AV} \tag{7}$$

where I, V, A, d are current, applied voltage, sample area and sample thickness respectively.

3.2   Dielectric spectroscopy and AC conductivity measurement
The dielectric properties as function of frequency were studied. The frequency varied in a controlled manner and all the data automatically collected. The measurements were carried out in the frequency range 10Hz to 100MHz, using a SR850 DSP Lock-In Amplifier, and the dielectric permittivity ε', ε'' and AC conductivity σac were calculated. The samples were prepared as discs of thickness about 0.5 mm and diameter of 10mm, with silver past electrodes on the opposite sites of the sample. The electrical contacts were formed by silver paint.

3.3 DSC analysis
DSC studies were carried out using differential scanning calorimeter equipped with an intercooler (Shimadzu DSC-60, Shimadzu Corporation, and Kyoto, Japan). Indium/zinc standard were used to calibrate the temperature and enthalpy scale. The samples were hermetically sealed in
an aluminum pans and heated at a constant rate of 10 °C/min over a temperature range of 25- 250 °C. Inert atmosphere was maintained by purging nitrogen gas at a flow rate of 50 ml/min.

3.4   SEM photomicrographs
Samples morphology was examined under scanning electron microscope (JEOL, JSM- 6360LV Scanning Microscope, and Tokyo, Japan). Before microscopy samples were sputter-coated using gold (JEOL, JFC-1100 fine coat ion sputter, Tokyo, Japan). The photomicrographs were taken at an acceleration voltage of 10 kV.

4. Results and discussion

4.1. DC Conductivity Measurements:
To evaluate the filler effect on the electrical conductivity of the composites, two procedures were employed including:
1. Applying a small DC potential on the test sample to avoid self heating effect
2. Left the field applied on test sample until the current become steady to avoid creep current due to static charge.
3. Use a suitable contact pressure by samples holder to avoid the effect of pressure on the conduction current.

Accordingly, the dependence of electrical resistively of the composites on CNP content is illustrated in Figure (1). It seems that the curve profile is characterized by a rapid increase in conductivity and gradual process approaching equilibrium with increasing conducting filler concentration. On the other hand, the critical filler fraction corresponding to the insulator–conductor transition, i.e., the percolation threshold, lies in about 0.08 vol. %. It is lower than the values of many conventional composites prepared by of single ready-made polymer and conductive fillers and also lower than other previous works [22]. The general theory to explain the conduction mechanism of fibers or particle-filled polymer composites is the theory of conductive paths [23, 24], which suggests that it is the existence of conductive paths (conducting particles) that results in the conductivity of the composites. With increasing the content of the filler, conductive paths among the fillers will increase. Also as suggested by Tchmutin et al. [25], the resultant intimate filler / matrix contacts further favour the injection of charge carriers from filler particles to polymer matrix. In contrast, it is difficult form a finely dispersed CNP nets in a ready made polymer matrix due the poor mobility of macro-molecules in the course of dispersive blending. Composites with low percolation threshold will favourites the practical application with regard to the less deteriorated mechanical properties and processability.
The percolation threshold in present work is about 0.08 volume fractions, which expected to be lower than that for PS/CNP composites fabricated by melt-mixing or by in-situ polymerization [22, 26]. This may attributed to the effect of sonication on the dispersion of CNPs. It is well known that the as-produced CNPs exist in an entanglement state. When dry powder of CNPs was directly mixed with molten PS, aggregates of CNPs could not be well disentangled because the interaction between PS molecule chains and CNPs was weaker than that between CNPs together [27]. When CNPs were sonicated in formalin, the CNPs entanglements turned loose or even disentangled because of the penetration of formalin molecules. To blend PS with CNPs in such a state, the dispersion of CNPs could be better, thus the pathway of conductive filler was easy to form and the percolation threshold of the composite was lower.
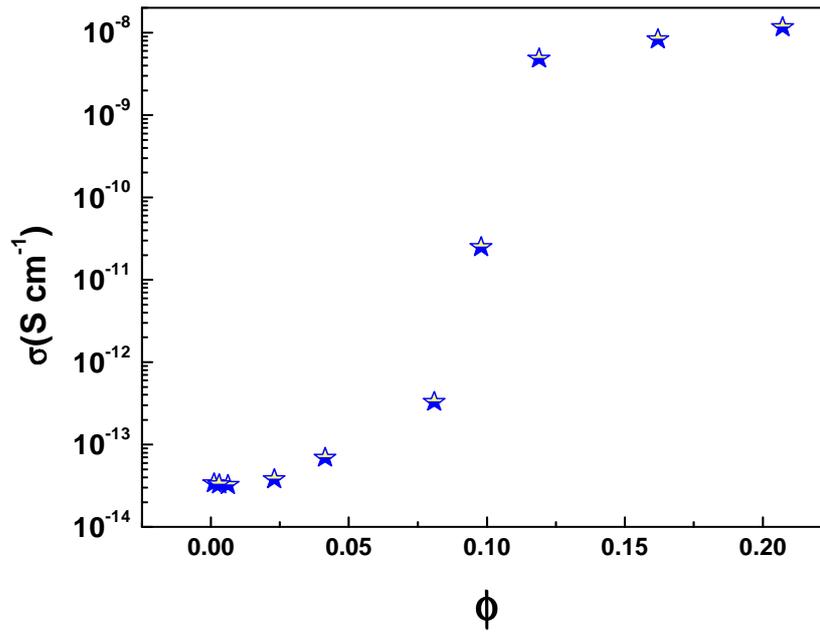
Fig. 1: Dependence of DC conductivity on volume fraction of CNPs

4.2 Dielectric and AC conductivity

Figure (2) shows variation of A.C. conductivity as a function of frequency for pure PS and CNP's composite (with different wt. %). At low frequencies, a frequency independent conductivity was recorded, which is attributed to resistive conduction through the bulk composite. On the other hand, at high frequencies (>100 up to 10^4Hz), conductivity appears to be proportional to frequency due to the capacitance of the host medium between the conducting particles or clusters of CNP. At higher frequencies (> 10^4Hz) a plateau region was recorded. This behaviour is the normal trend or polystyrene film [28].
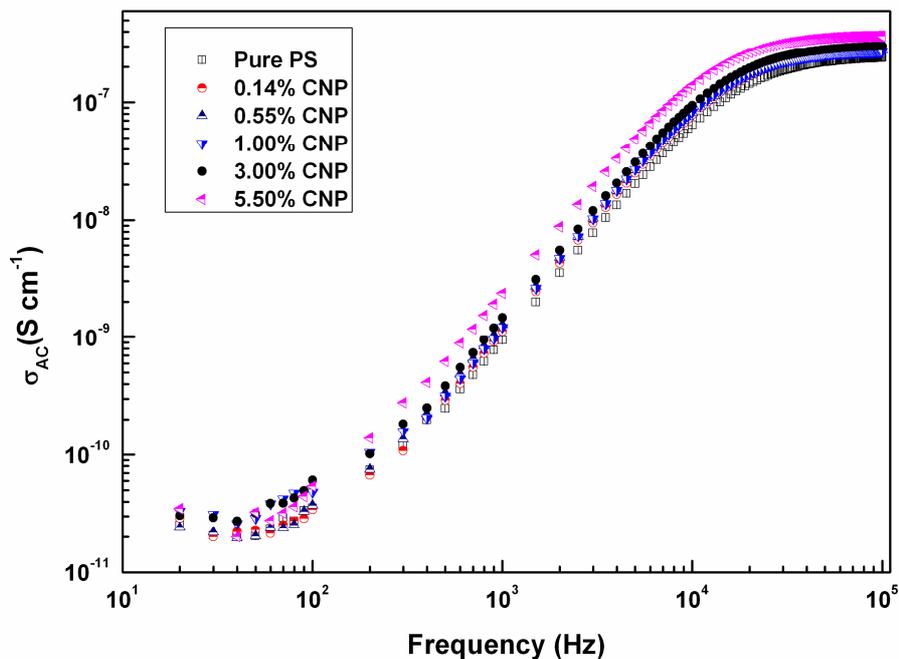
Fig. 2: Frequency dependence of σ_{ac} for PS/CNPs nanocomposite

121

Figure (3) shows variation of dielectric permittivity (real part) as a function of frequency for pure PS and CNP's composite. It is observed that at low frequencies dielectric constant was found to be frequency independent, then above 10^4 Hz dielectric permittivity decreased with increasing frequency. The behavior for PS is a good agreement with the previous data [28]. It is expected that there are no any kind of interaction between polystyrene polymer and carbon nanoparticles since the behaviour not suffer any change even for high loading of CNP. The trend can be interpreted by assuming the electronic model consists of two conductance and capacitance as shown in figure (4).
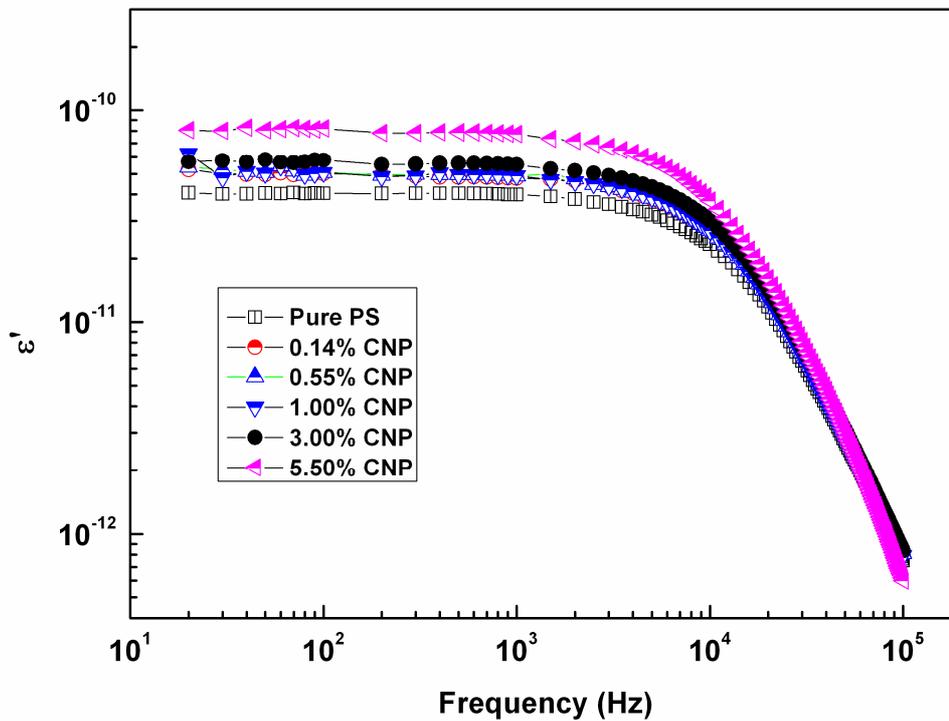

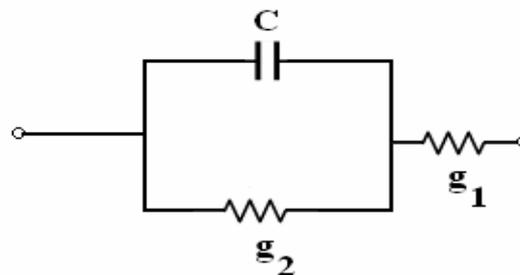**Fig. 3:** Frequency dependence of ε' for PS/CNPs nanocomposite

Fig. 4: Equivalent circuit model for ε' behaviour for PS/CNPs nanocomposite.

The variation in ε' may be attributed to the interfacial conductance g_1 between the polymer and carbon nanoparticles.

Figure (5) shows variation of dielectric loss as a function of frequency. It is observed that ε'' in case of PS and its composite gives a beak value near 10^4Hz. This peak represents α relaxation for polystyrene that occurs at kilohertz frequency region [29]. By the same manner the data indicates that there was no type of interaction between polymer matrix and nanoparticles.
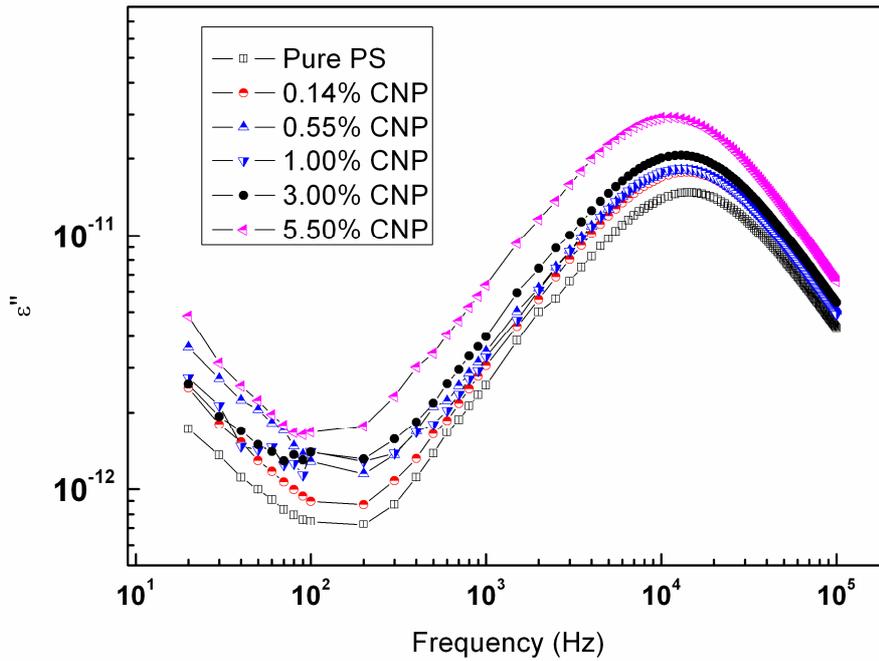
Fig. 5: Frequency dependence of ε" for PS/CNPs nanocomposite

4.3 I-V characteristics

Figure (6) and (7) illustrates I-V and log I -log V plots for PS/CNP composites with different weight ratio. It is clearly seen that the I-V relationship is not linear relation. While the Log (I)-log (V) relation was nonlinear for pure and low weight ratio composite while above percolation threshold it becomes linear relationship. This result indicates the interconnection and network formation for CNPs through host polymer above percolation threshold.

I -V characteristics can be expressed as [30]

$$I(\phi,V) = K(\phi).V^n \qquad (8)$$

Where K (φ) represents the conductivity of the composite at a given value of φ and n is the slope in the log I - log V plot. In equation (3), Ohm's law is fulfilled in the system at n = 1.
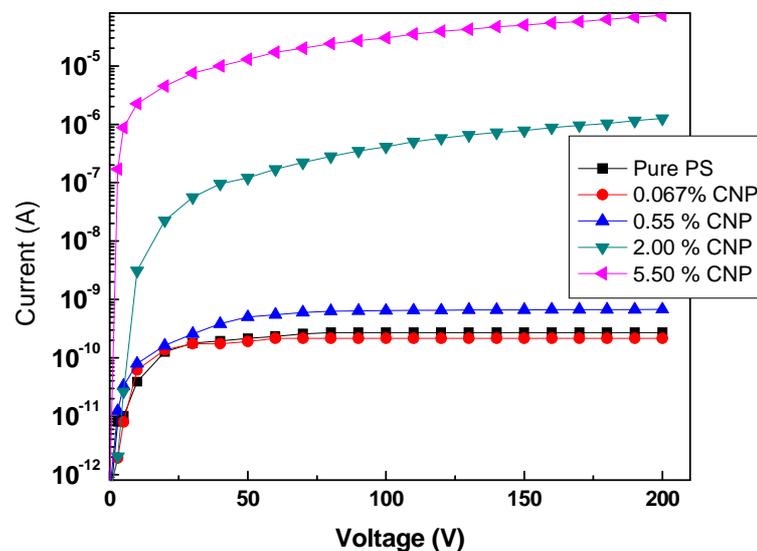

Fig. 6: I-V characteristic curves for pure PS and PS/CNPs nanocomposite film**.**

123

It was found that the value of n = 1.17 at ϕ_c and it decreased to 1 at $\phi \sim 0.071$. This indicate that the transition from insulator phase to conducting phase start at 0.071 volume fraction. The transition of the conduction mechanism from non-linear (insulator) to Ohmic (conductor) is generally understood in terms of distance and number of tunneling gaps in the percolating network [31] and the tunneling gaps start to change into Ohmic contacts.
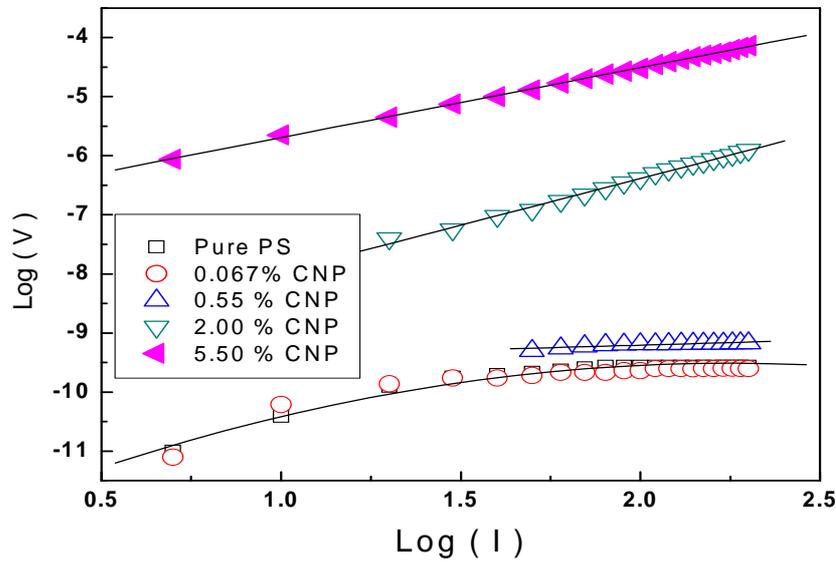

Fig. 7: log(V)-log(I) relationship for pure PS and PS/CNPs nanocomposite film

4.4 DSC Data Analysis:

Figure (8) shows the DSC curves of pure polystyrene and PS/CBNP nanocomposite measured at a scanning rate of 10 C/min. The glass transition temperature of pure polystyrene was found to be 91.4°C. T_g was defined as the temperature at the median point in the range of glass transition during the heating process. The step change of the DSC curves was not detected for composite samples but a discontinuity in the slope of the heat flow vs. temperature plot was observed. These discontinuities appear to be attributable to glass transition.
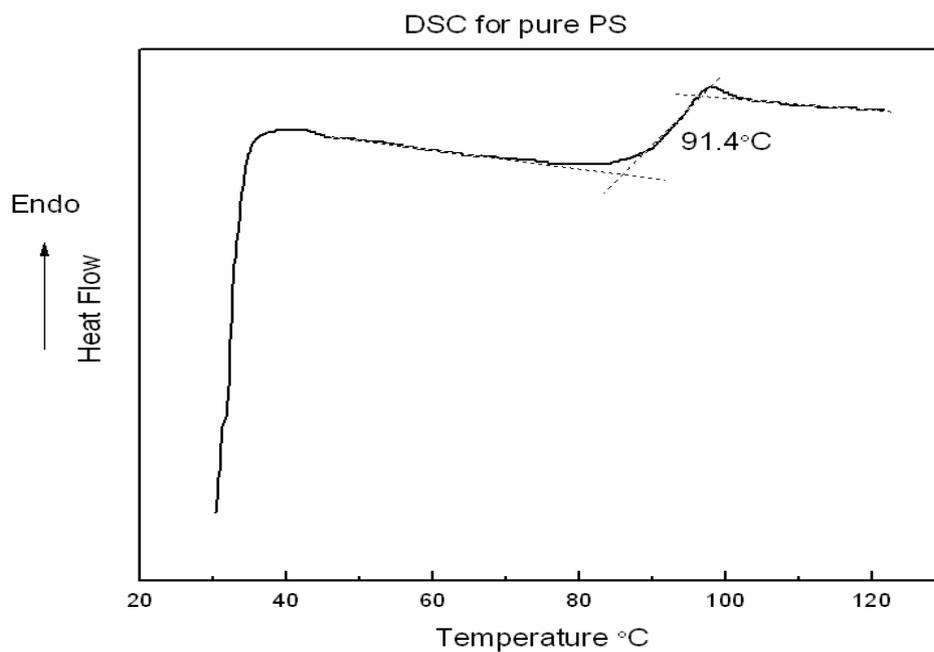

Fig. 8: DSC curve for pure PS film.

The estimated values of T_g's were determined from the intersection point of the two linear region (Figure 9) listed in Table 1. The incorporation of CBNP with 0.05wt%, reduces the Tg of polystyrene to ≈ 86 °C. The extent of decrease in Tg was more pronounced in the case of 0.55wt% of CBNP composite sample (≈ 67 °C) and may be attributed to the improved plasticization effect of CBNP's. Xin Lan et al.[32], study thermoset styrene-based shape-memory polymer (SMP) filled with carbon black and they reported that T_g decreases slightly with the increase of CNP volume fraction. This shift of T_g to lower temperature may be attributed to, the increase in amorphous state in the composite since the crosslink cause shifting in T_g to higher temperature [33] , or to the plasticization effect of the nano-filler.
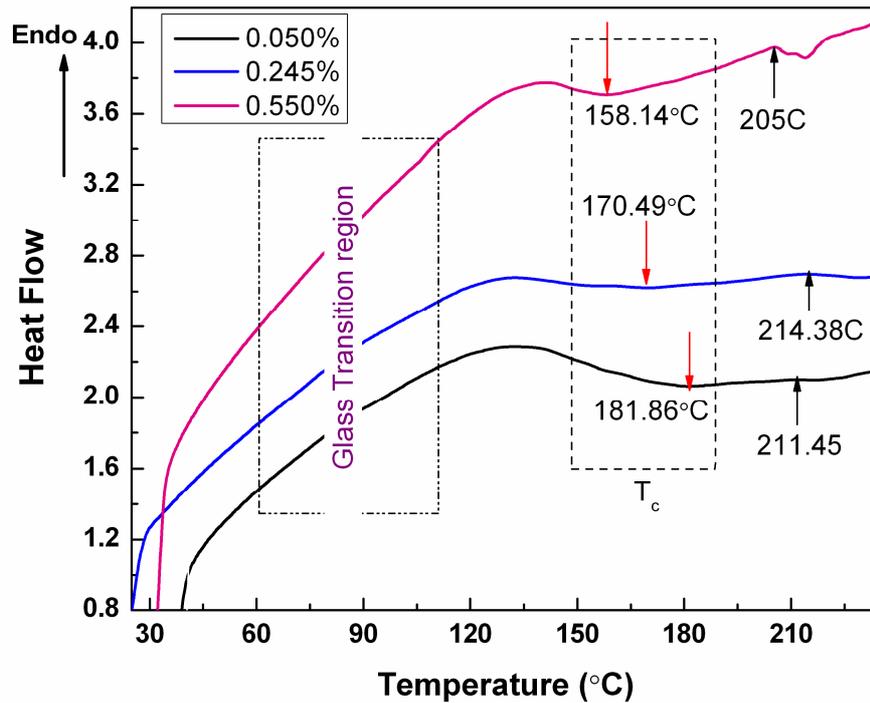

Fig. 9: DSC curves for PS/CNPs nanocomposite

Table 1: The glass transition temperatures (T_g) measurements results for PS/CNPs nanocomposite

CBNP wt%	Tg(°C)	T_C(°C)
0.050	86.37	181.86
0.245	84.82	170.49
0.550	67.52	158.14

4.5 SEM analysis:

It is well established that the resistivity and percolation threshold of CNPs-filled single polymers depend greatly on the interaction of the polymer and CNPs and the CNPs distribution [35-37]. The difference in the percolation thresholds of the carbon nanoparticles polymer composites can be explained by the morphological differences. Figure 10-A shows the scanning electron microscopy (SEM) micrographs for 0.067 wt% CNP/PS sample. The particles are appearing to be separate and no aggregation was formed. In figure 10-B (1%CNPs/PS) the aggregate was formed as cluster with branches. The distribution of CNP in PS was relatively homogeneous for low concentration and cluster formation will cause the threshold percolation.
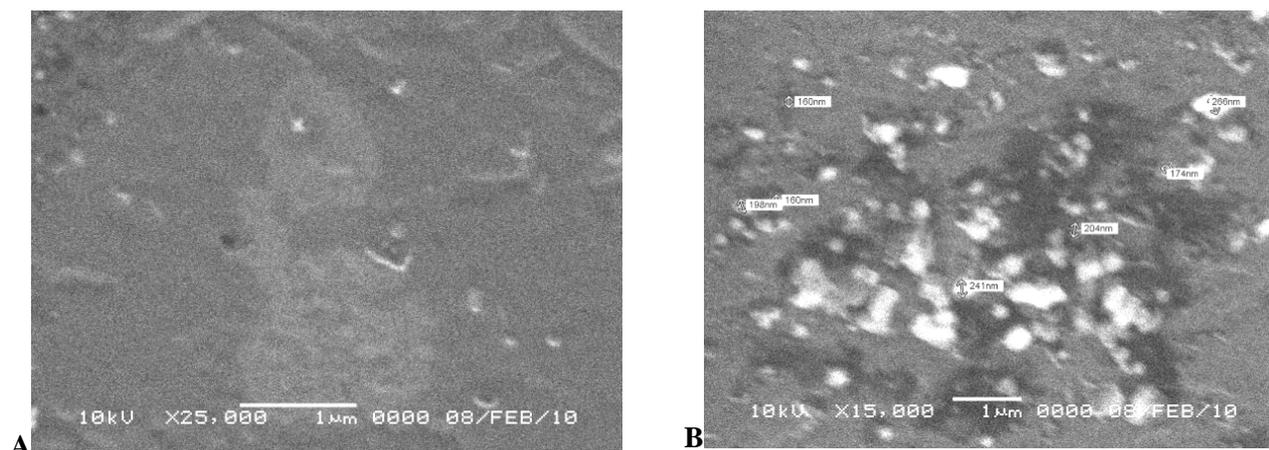
Fig. 10: SEM micrographs of (A) 0.067wt.% and (b) 1wt.% CNPs/PS samples

Conclusion

Conductive polymer composites exhibiting a reduced percolation threshold have been successfully prepared by the incorporation of CNP into PS polymer matrix. The CNP- filled PS composite exhibits low electrical resistivity. The composite has a percolation threshold of 2%wt% of CNPs, which is lower than reported in literatures. From dielectric measurements, It is expected that there are no any kind of interaction between polystyrene polymer and carbon nanoparticles. Dielectric trend interpreted by assuming the electronic model consists of two conductance and capacitance model. The α relaxation peak for polystyrene was appeared at kilohertz frequency region. Log(I)-log(V) relation was nonlinear for pure and low weight ratio composite while above percolation threshold it becomes linear relationship. The incorporation of CNPs with 0.05wt%, reduces the T_g of polystyrene to 86 °C. The extent of decrease in T_g was more pronounced in the case of 0.55wt% of CNPs composite sample (67°C) and may be attributed to the improved plasticization effect of CNP's. Scanning electron microscopy (SEM) micrographs shows aggregate formation at the threshold concentration.

Acknowledgement

References

1. Encyclopedia of composite materials and components. 1986.
2. Maclaga, B., Fisher, W. K. *Text. Res. J.* 71(2001) 281.
3. Dhawan, S.K., Singh, N., Rodrigues, D. *Adv. Mat.* 4 (2003) 105.
4. Wang, L., Tay, B. See, K., Sun, Z., Tan, L., Wang, D. *Carbon* 47(2009) 1905.
5. Ma, P., Siddiqui, N., Marom, G., Kim, J. A review, *Composites Part A: Applied Science and Manufacturing 41* (2010) 1345.
6. Liang, J., Wang, Y., Huang, Y., Ma, Y., Liu, Z., Cai, J., Zhang, C., Gao, H., Chen Liang, Y. *Carbon* 47 (2009) 922.
7. Pande, S., Singh, B., Mathur, R. *Nanoscale Res. Lett.* 4 (2009) 327.
8. Heiser, J., King, J., Konell, J, Sutter, L. *Poly. Compos.* 25 (2004) 407.
9. Kara, S., Arda, E., Dolastir, F., Pekcan, Ö. *J. Colloid and Interface Science* 344 (2010) 395.
10. Spitalsky, Z., Tasis, D., Papagelis, K., Galiotis, C. *Progress in Polymer Science* 35 (2010) 357.
11. Sun, G., Chen, G., Liu, Z., Chen, M. *Carbon* 48 (2010) 1434.

12. Gavrilov, N., Okotrub A., Bulusheva, L., Sedelnikova, O., Yushina I., Kuznetsov V. *Composites Science and Technology* 70 (2010) 719.
13. Chen, S., Hu, J. , Zhang, M. , Rong, M. , and Zheng, Q. *Sens Actuators, B*, 113 (2006) 361.
14. Richner, M., Wokaun, A., *Carbon* 40 (2002) 307.
15. Sudha, J., Sivakala, S., Patel, K., Radhakrishnan Nair, P. *Composites Part A: Applied Science and Manufacturing* 41 (2010) 1647.
16. Zhang, C, Han, H., Yi, X., Asai, S., Sumita, M. *Compos Interface* 6 (1999) 227.
17. Lu, G., Li, X., jiang, H., Mao, X., *J. Appl. Polym. Sci*. 62 (1996) 2193.
18. Thongruang, W., Spontak, R., Maurice, C., *Polymer* 43 (2002) 2279.
19. Kirkpatrick, S. *Rev. Mod. Phys*. 45 (1973) 574.
20. Zallen, R., The Physics of Amorphous Solids., New York, Jhon Wiley & Sons (1983)
21. Ibrahim, S., Ayesh, A., Al-Shoaibi, A. *J. Thermoplastic Composite Materials* 22 (2009) 335.
22. Rong Li, J., Rui Xu, J., Qiu Zhang, M. , Zhi Rong, M. *Carbon* 41 (2003) 2353.
23. Miyauchi, S., Togashi, E., *J. Appl. Polym. Sci.* 30 (1985) 2743.
24. Poiiey, M., Boonstra, B., Rubb. *Chem. Technol.* 30 (1957) 170.
25. Chmutin, L., Shevchenko, V., Ponomarenko, A., Klason, C. In: Abstracts of the 5th international conference on composite interfaces, Gothenburg; 20–24 June (1994) 29.
26. Zaragoza-Contreras , E., Hernández-Escobar, C., Navarrete-Fontes AFlores - Gallardo., S. *Micron* 42 (2011) 263.
27. Tang, W., Santare, M., Advani, S., *Carbon* 41 (2003) 2779.
28. Terry, C., Hans, G., Jeffrey, L. *American Laboratory, Technical Articles* April (2010)
29. Roldán-Toro, R., Solier, J. D. *Journal of Colloid and Interface Science* 274 (2004) 76.
30. Mamunya, Y., Muzychenko, Y., Pissis, P., Lebedev, E., Shut, M., *Polym. Eng. Sci.* 42 (2002) 90.
31. Nakamura, S., Saito, K., Sawa, G., Kitigawa, K., *Jpn. J. Appl. Phys.* 36 (1997) 5163.
32. Lan, X., Leng, J., Liu,Y., Du, S. *Advanced Materials Research* 47 (2008) 714.
33. Ming, Lu, Zhou, J., Wang, L., Zhao, W., Lu, Y., Zhang, L., Liu, Y. J. *Nanomaterials*, 2010(2010)1.
34. http://www.qrins.com/ckseo/ed/paper/Paper%20For%20Puplication%20In%20American%20Laboratory.pdf
35. Cheah, K., Forsyth, M., Simon, G. P., J Polym Sci Part B: Poly. Phys. 38 (2000) 3106.
36. Mironi-Harpaz , I., Narkis, M., *J Appl Poly. Sci.* 81 (2001) 104.
37. Li, Y., Wang, S., Zhang, Y., Zhang, Y., *J App. Pol. Sci.* 98 (2005) 1142.